Electronic Supplementary Material (ESI) for Chemical Science.
This journal is © The Royal Society of Chemistry 2021

Supporting Information for

Synergistic Enhancement for Emergency Treatment Effect of Organophosphate Poisoning by A Supramolecular Strategy

Junyi Chen,‡[ab] Yadan Zhang,‡[a] Yao Chai,[a] Zhao Meng,[a] Yahan Zhang,[a] Longming Chen,[a] Dongqin Quan,*[a] Yongan Wang,*[a] Qingbin Meng*[a] and Chunju Li*[c]

[a] State Key Laboratory of Toxicology and Medical Countermeasures, Beijing Institute of Pharmacology and Toxicology, Beijing 100850, P. R. China.

[b] College of Environmental and Chemical Engineering, Shanghai University, Shanghai University, Shanghai 200444, P. R. China.

[c] Key Laboratory of Inorganic-Organic Hybrid Functional Material Chemistry, Ministry of Education, Tianjin Key Laboratory of Structure and Performance for Functional Molecules, College of Chemistry, Tianjin Normal University, Tianjin 300387, P. R. China.

Table of Contents

1. General materials and methods

1.1 Materials. All reagents were purchased commercially and used without further purification unless otherwise noted. Acetylcholine chloride (ACh) and pyridine-2-aldoxime methochloride (PAM) were purchased form Tci. Acridine Orange (AO) was form Alfa Aesar. Acetylcholinesterase (AChE) was form Ruitaibio. Dulbecco's modified eagle medium (DMEM) was purchased from Thermo Fisher Scientific. Fetal bovine serum (FBS), penicillin-streptomycin and PBS were purchased from Invitrogen. The cell counting kit-8 (CCK-8) was from Dojindo. The mouse brain microvascular endothelial cells (bEnd.3) were obtained from the cell bank of Chinese Academy of Sceinence.

1.2 Instruments. ^{1}H and ^{13}C NMR data were recorded on a JNM-ECA-400 spectrometer, JEOL Ltd. Fluorescence spectroscopic studies were carried out by a LS-55 fluorescence spectrophotometer, PerkinElmer, Inc. Fluorescence imaging were recorded by IVIS Spectrum system, PerkinElmer, Inc. Cytotoxicity studies were performed on SpectraMax ® M5 plate reader, Molecular Devices. Histological analysis was examined on VS200 digital scanning system, Olympus, Inc.

1.3 Cell and Animals. bEnd.3 cells were cultured in DMEM supplemented with 10% FBS, 1% penicillin and 1% streptomycin. Then cells were incubated at 37 ^{o}C under 5% CO_2 and 90% relative humidity, and passaged every 2 days.

Sprague-Dawley (SD) rats (200 ± 20 g) of both sexes were purchased from SPF Biotechnology Co., Ltd. (Beijing, China) and maintained at 25 °C in a 12 h light/dark cycle with free access to food and water. Animals were allowed to acclimate to environment for at least one week before experiments. All experimental procedures were conducted in accordance with the Guide for the Care and Use of Laboratory Animals of the AAALAC, and were approved by the Animal Care and Use Committee of the National Beijing Center for Drug Safety Evaluation and Research. Best efforts were made to minimize the number of animals used and their suffering.

1.4 NMR spectroscopy. Samples of M, CP5A and CP6A for NMR measurement were prepared in D_2O. Samples for 1:1 ^{1}H NMR spectra were prepared in PD 7.4 deuterated

phosphate buffer (10 mM). All NMR spectra were acquired at 298 K in the solution state.

1.5 Fluorescence titration. As reported previously,[1] to quantitatively assess the complexation behavior of these compounds, fluorescence titrations of hosts with guests were performed at 298 K in a phosphate buffer solution of pH 7.4 by equation 1. We considered that a host formed a 1:1 host:guest complex with a guest at an association constant (K_a), which satisfied the respective law of mass action relating to the equilibrium concentrations of free host ([H]), free guest ([G]) and host-guest complex ([HG]). The relationship between the total concentration of host ($[H]_0$), guest ($[G]_0$) and their equilibrium concentrations were introduced by the law of mass conservation (equation 2-1 and 2-2). Here $[H]_0$ was the initial concentration of guest as a known parameter, which was kept constant in the titration process. Then equation 1 and 2-2 were employed to deduced equation 3. When the fluorescence titration was performed, the intensity of fluorescence (F) corresponded to the combined intensity of the host and the host-guest complex, which were described by molar fractions (equation 4). Both F_{HG} and F_H were known parameters in which F_H was the fluorescent of $[H]_0$ and F_{HG} was the fluorescent intensity when all host were complexed. The equation 5 deduced by equation 2-1, 2-2, 3 and 4, explained the relationship between K_a and variables $[G]_0$ in fluorescence titration.

$$[H] + [G] \overset{K_a}{\leftrightarrow} [HG]$$

$$K_a = \frac{[HG]}{[H][G]} \quad (1)$$

$$[G] = [G]_0 - [HG] \quad (2\text{-}1)$$

$$[H] = [H]_0 - [HG] \quad (2\text{-}2)$$

$$[HG] = \frac{K_a[G][H]_0}{1 + K_a[G]} \quad (3)$$

$$F = \frac{[HG]}{[H]_0}F_{HG} + \frac{[H]}{[H]_0}F_H \quad (4)$$

$$F = F_{HG} + (F_H - F_{HG})\frac{\left([H]_0 - [G]_0 - \frac{1}{K_a}\right) - \sqrt{([H]_0 - [G]_0 - \frac{1}{K_a})^2 + 4[G]_0[H]_0}}{2[H]_0} \quad (5)$$

1.6 Patch-clamp recording of nAChR-activated whole-cell responses. HEK293

cells were used to express nicotinic acetylcholine receptor α7 subunit CHRNA7. Cells were incubated with DMEM supplemented with 10% FBS, 800 μg·mL^{-1} G418 and 200 μg·mL^{-1} Hygromycin B at 37 ^{o}C under 5% CO_2 and 90% relative humidity. Then Cells were detached from the flask with 0.25 % Trypsin-EDTA and seeded on glass slides into 24-well plate at a density of 8 × 10^3 cells/well.

The application of pressure for forming gigaseals and the whole-cell patch clamp configuration were established using motorized micromanipulator (Sutter Instruments, USA). During whole-cell recording, the membrane potential was held at -70 mV. All data were analyzed using ParchMaster softerware (HEKA, Germany).

The solution used:

Extracellular: 140 mM NaCl, 3.5 mM KCl, 2 mM $CaCl_2{\cdot}2H_2O$, 1 mM $MgCl_2{\cdot}6H_2O$, 10 mM HEPES, 10 mM D-Glucose, 1.25 mM NaH_2PO_4. Titrate to pH 7.4 at 25 ^{o}C with NaOH.

Intracellular: 50 mM CsCl, 10 mM NaCl, 20 mM EGTA, 60 mM CsF, 10 mM HEPES. Titrate to pH 7.4 at 25 ^{o}C with CsOH.

1.7 Fluorescence imaging. 1.00 mM ACh was added to the AO/CP6A (10/50 μM) in rat cerebrospinal fluid at 25 ^{o}C and stirred for 30 min to measured signal intensity, where the radiance of AO/CP6A (10/50 μM) as control.

The SD rats were randomly divided into 2 groups: non-poisoning and POX-poisoned group (0.8 × LD_{50} of POX, 600 μg·kg^{-1}, *i.p.*). 1 h after poisoning, rats of both groups were administrated with 20 μL of AO/CP6A (10/50 μM, *icv*). For investigating *ex vivo* fluorescence recovery by the displacement of ACh, the rats were sacrificed after 0.5 h injection and brains were collected and subjected for *ex vivo* imaging. The excitation wavelength was 490 nm and spectral imaging at 530 nm was carried out. We acquired the image data sets and measured the signal intensity using region-of-interest analysis with the Living Image software (Xenogen) and normalized the images displayed on each data set according to color intensity.[2]

1.8 Safety and biocompatibility of CP6A. The relative cytotoxicity of CP6A against bEnd.3 cells was assessed *in vitro* using CCK-8 according to the manufacture's instruction. bEnd.3 cells were seeded into 96-well plates at a density of 8000 cells/well

in 100 μL of DMEM supplemented with 10% FBS, 1% penicillin, and 1% streptomycin and cultured for 24 h in 5% CO_2 at 37 °C. CP6A was dissolved in PBS and then diluted to the required concentration. It was then added to the cell-containing wells which were further incubated at 37 °C under 5% CO_2 for 72 h. Subsequently, 10 μL of CCK-8 was added into each well and incubated for another 0.5 h. The plates were then measured at 450 nm using a plate reader. All experiments were carried out five independent times. Cell viability was calculated as follows:

$$Cell\ Viability = \frac{OD_{test} - OD_{blank}}{OD_{control} - OD_{blank}} \times 100\%$$

T

Where OD_{blank} is the optical density of blank well (medium and CCK-8 reagent), OD_{test} is the optical density of the test group and $OD_{control}$ is the optical density of the control group.

To verify the safety of CP6A against brain tissue, SD rat swere intranasally administered with CP6A at a dose of 190 mg·kg^{-1}. After 72 h, the rats were sacrificed and the brains were separated from the animals. Then brains were fixed in glutaraldehyde (3%) for 48 h. After dehydration and embedding, the tissue was cut into 4 μm sections and stained with hematoxylin and eosin. The images were then acquired by a digital scanning system.

1.9 Assay of PAM in cerebrospinal fluid. Briefly, 10 mg·kg^{-1} free PAM, 96 mg·kg^{-1} M + 10 mg·kg^{-1} PAM (molar ration = 6), 79 mg·kg^{-1} CP5A + 10 mg·kg^{-1} PAM (molar ration = 1) and 95 mg·kg^{-1} CP6A + 10 mg·kg^{-1} PAM (molar ration = 1) were administrated intranasally in SD rats at predetermined time intervals (10 min and 30 min after administration). After that, rats were anesthetized and placed on the operating table in a prone position and 0.1mL cerebrospinal fluid was collected through the foramen occipital magnum with an intravenous needle. The collected cerebrospinal fluid was centrifuged (5000 g, 5min, 4 ^{o}C) and the content of PAM were analyzed using HPLC method. The column used was a C18 reverse-phase column (SHISEDO, 250*4.6 mm), and the mobile phase for elution consisting of 10 mM sodium n-heptanesulfonate and 0.12% trifluoroacetic acid with acetonitrile (94:6 v/v). The injection volume and

flow rate was set as 20 μL and 2.0 mL/min, respectively. The eluent was monitored at 294 nm at 30°C.

1.10 Measurement of AChE viability, inhibition and reactivation level. For the *in vivo* brain relative AChE viability assay, PBS (control), 96 mg·kg^{-1} M, 79 mg·kg^{-1} CP5A and 95 mg·kg^{-1} CP6A were administrated intranasally to SD rats. Whole brains were collected 30 min after administration and frozen in liquid nitrogen. Thereafter AChE concentration of brain homogenates was analyzed and relative AChE viability was defined as follows:

$$Relative\ AChE\ viability = \frac{AChE\ content\ in\ experiment\ group}{AChE\ content\ in\ control\ group} \times 100\%$$

For the *in vivo* brain AChE inhibition assay, brains of control group rats were collected 1 h after *i.p.* injection of PBS and then 10 min or 30 min after intranasal administration of PBS. Other rats were poisoned by 0.8 × LD_{50} of POX (600 μg·kg^{-1}, *i.p.*), 1 h after POX administration rats were intranasally administrated 96 mg·kg^{-1} M, 79 mg·kg^{-1} CP5A and 95 mg·kg^{-1} CP6A. Whole brains were then collected 10 min or 30 min after administration and frozen in liquid nitrogen. Thereafter AChE concentration of brain homogenates was analyzed and relative AChE inhibition was defined as follows:

$$AChE\ inhibition = 1 - \frac{AChE\ content\ in\ experiment\ group}{AChE\ content\ in\ control\ group} \times 100\%$$

For the *in vivo* brain AChE reactivation assay, brains of control group rats were collected 1 h after *i.p.* injection of PBS and then 10 min or 30 min after intranasal administration of PBS. Other rats were poisoned by 0.8 × LD_{50} of POX (600 μg·kg^{-1}, *i.p.*), 1 h after POX administration rats were intranasally administrated 10 mg·kg^{-1} free PAM, 96 mg·kg^{-1} M + 10 mg·kg^{-1} PAM (molar ration = 6), 79 mg·kg^{-1} CP5A + 10 mg·kg^{-1} PAM (molar ration = 1) and 95 mg·kg^{-1} CP6A + 10 mg·kg^{-1} PAM (molar ration = 1). Whole brains were then collected 10 min or 30 min after administration and frozen in liquid nitrogen. Thereafter AChE concentration of brain homogenates was analyzed and relative AChE reactivation effieciency was defined as follows:

$$Reactivation\ Efficiency = 1 - \frac{AChE\ inhibition\ in\ treated\ group}{AChE\ inhibition\ in\ untreated\ group} \times 100\%$$

Whole brain homogenates were prepared in a tissue homogenizer with PBS at 4 ^{o}C and then samples were incubated with ACh (final concentration 10 mM) at same volume. After incubation at 37 ^{o}C for 45min, reaction was stopped by 30% acetonitrile and 10% trifluoroacetic acid to precipitate protein. Samples were centrifuged at 4 °C (5000 g, 5 min), and then supernatants were collected for analysis. AChE concentration was indicated in relation to the consumption of ACh, which was measured using HPLC. The column used was a C18 reverse-phase column (SHISEDO, 250*4.6 mm), and the mobile phase for elution consisting of 5mM sodium n-heptanesulfonate and 0.12% trifluoroacetic acid with acetonitrile (90:10 v/v). The injection volume and flow rate was set as 20 μL and 1.5 mL/min, respectively. The eluent was monitored at 205 nm at 30°C. Calibration curve was obtained through a similar procedure that a series of standard AChE solution (0.5, 1, 2, 3, 4 mg·mL^{-1}) reacted with 10 mM ACh at 37 °C for 45min and the resulting samples were determined by above HPLC method.

1.11 POX toxicity shift assay and histological analysis of brain sections. For the POX toxicity shift assay, 10 mg·kg^{-1} free PAM, 96 mg·kg^{-1} M + 10 mg·kg^{-1} PAM (molar ration = 6), 79 mg·kg^{-1} CP5A + 10 mg·kg^{-1} PAM (molar ration = 1) and 95 mg·kg^{-1} CP6A + 10 mg·kg^{-1} PAM (molar ration = 1) were administrated intranasally against 2 × LD_{50} of POX (1500 μg·kg^{-1}, *i.p.*). The ratio of surviving rats after challenge with POX and alleviation situation of POX-induced generalized seizures/status epileptics (SE) were used as a criterion of the toxicity shift. Behavioral seizures were classified according to the Racine Scale: stage 1, mouth and facial movements; stage 2, head nodding; stage 3, forelimb clonus; stage 4, rearing; stage 5, rearing and falling.[3] Onset of SE was determined by the presence of continuous stage 3 and above level seizures, which were objectively and independently determined by three trained observers.

For histological analysis of brain sections, brain of rats in the different groups were collected and fixed in 4 % paraformaldehyde, and then paraffin embedded sections were conducted for hematoxylin and eosin (H&E) staining. The samples were examined by a digital scanning system.

1.12 Statistical analysis. Quantitative data were expressed as mean ± SD. ANOVA and Student's t test were utilized for statistical analyses.

2. Syntheses of M, CP5A and CP6A

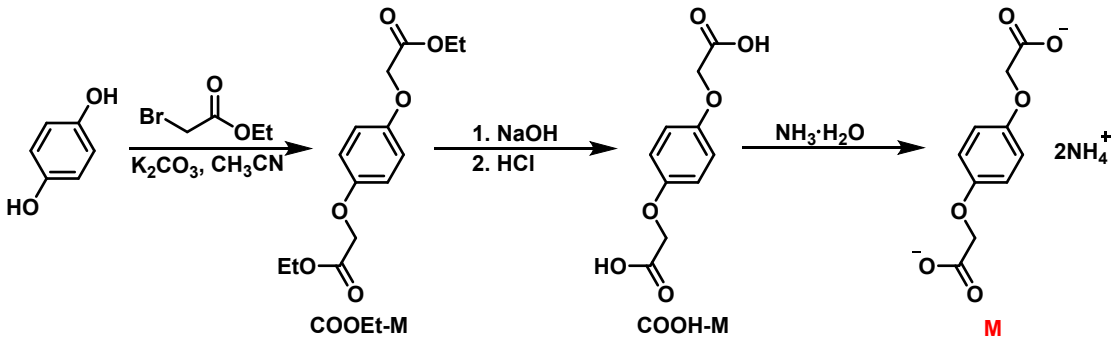

Scheme S1. Synthetic routes of M.

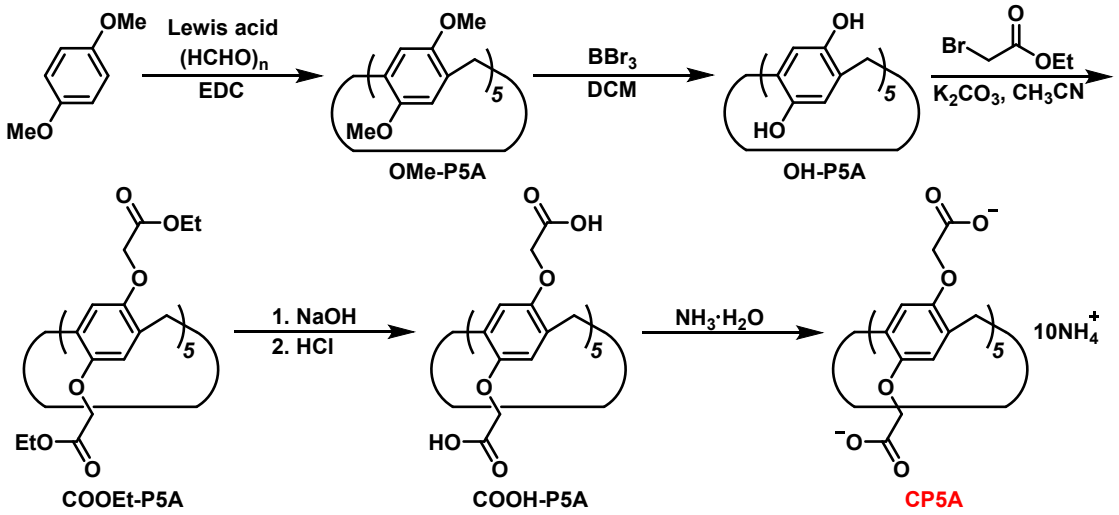

Scheme S2. Synthetic routes of CP5A.

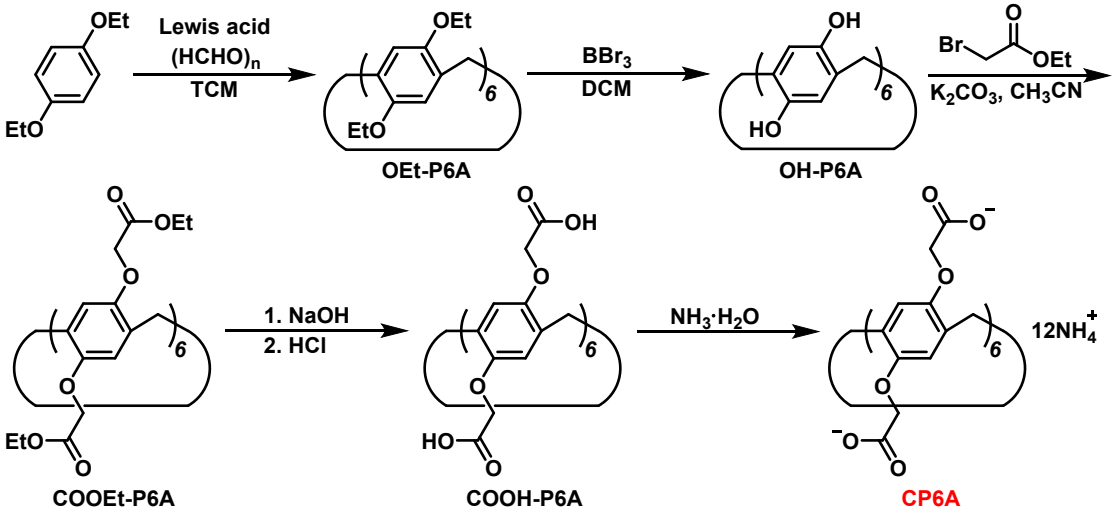

Scheme S3. Synthetic routes of CP6A.

M, CP5A and CP6A were synthesized and purified according to the procedure

reported previously.[4]

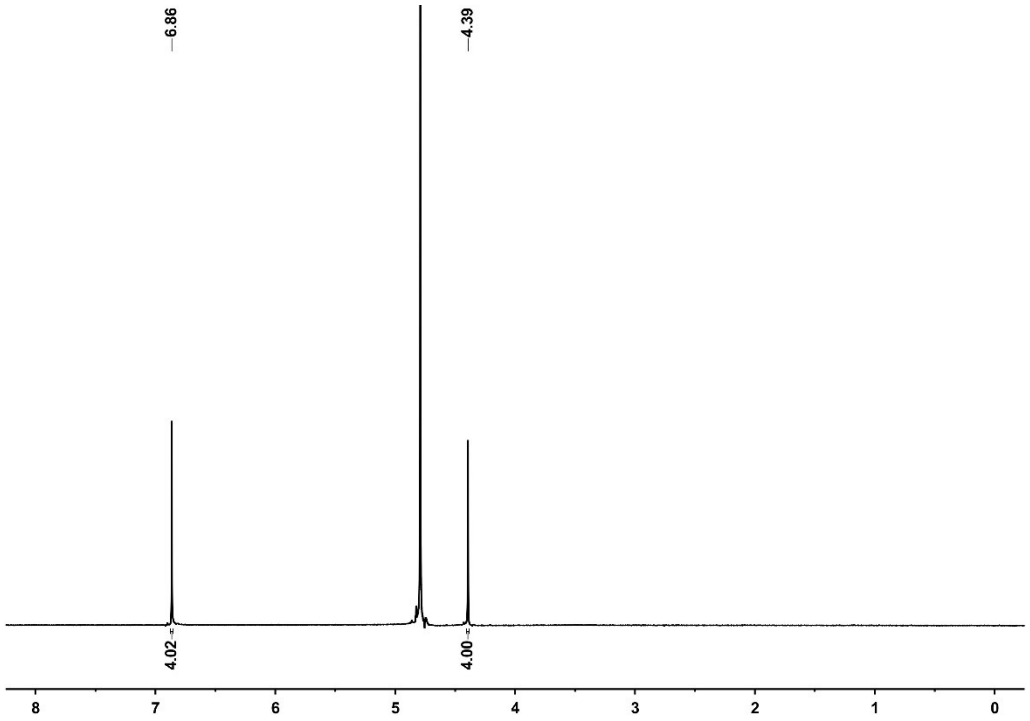

Fig. S1. ^{1}H NMR spectrum of M in D_2O, 400 MHz.

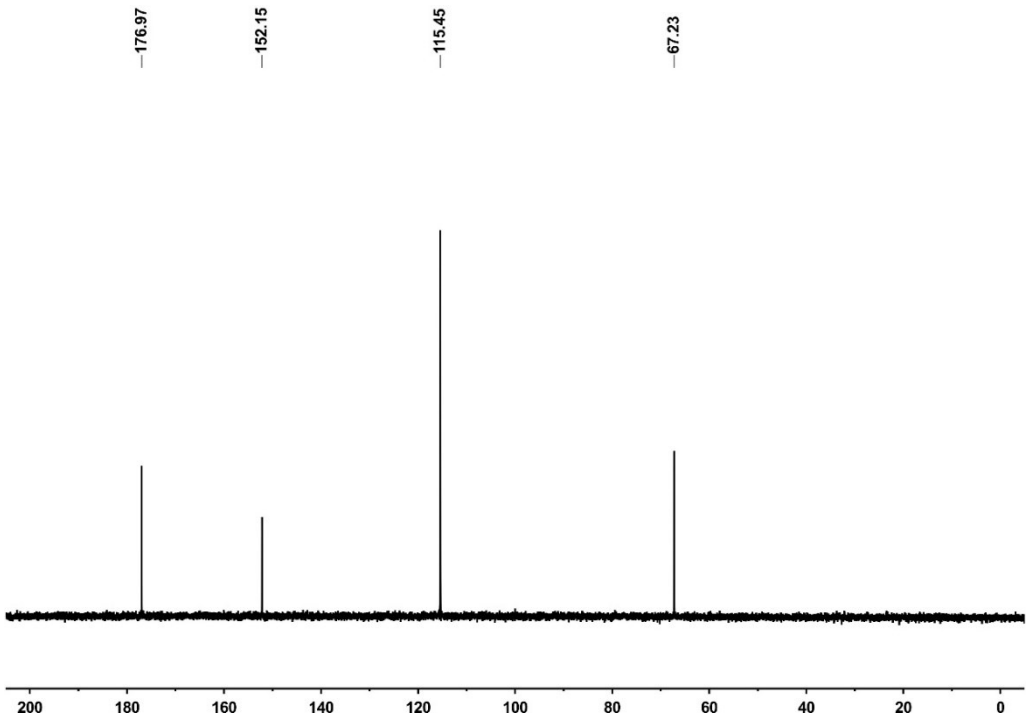

Fig. S2. ^{13}C NMR spectrum of M in D_2O, 100 MHz.

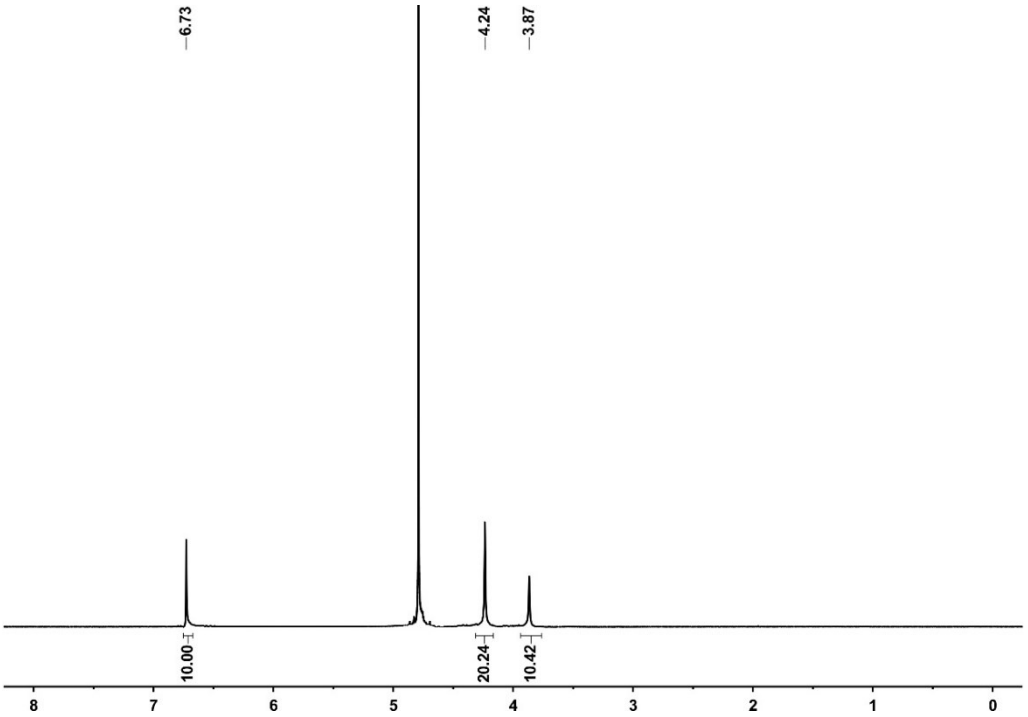

Fig. S3. ^{1}H NMR spectrum of CP5A in D_2O, 400 MHz.

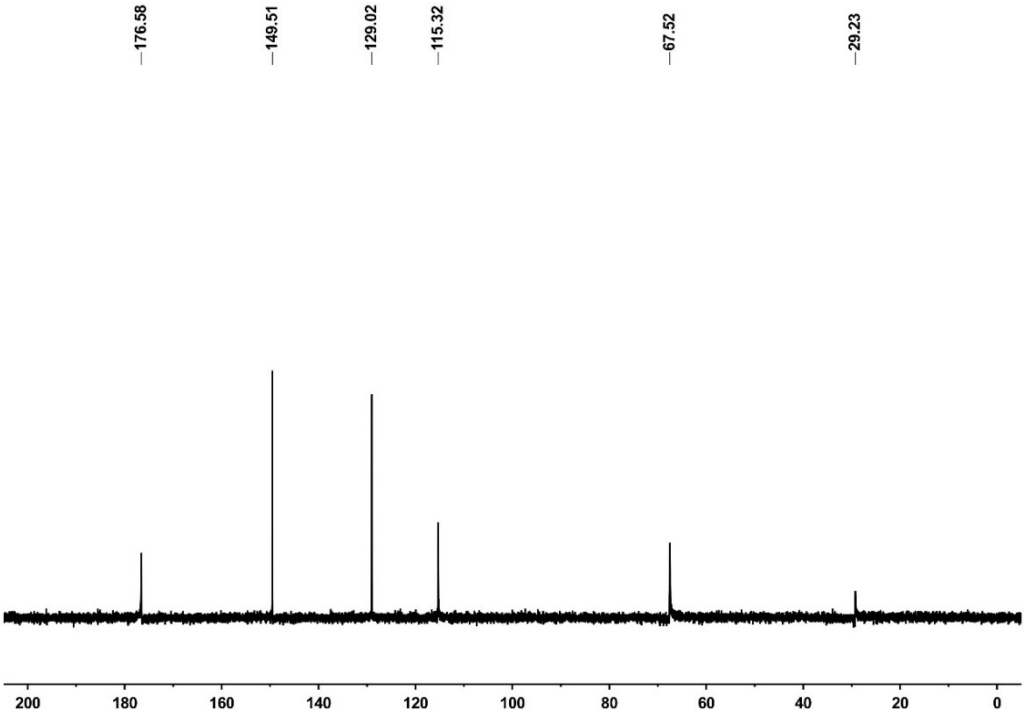

Fig. S4. ^{13}C NMR spectrum of CP5A in D_2O, 100 MHz.

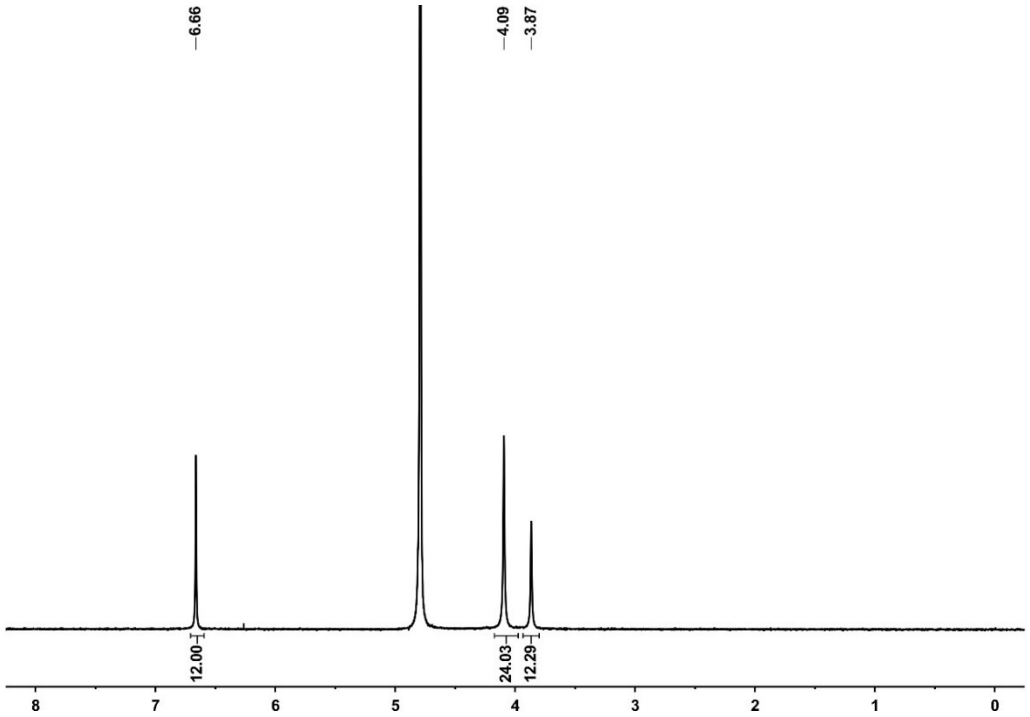

Fig. S5. ^{1}H NMR spectrum of CP6A in D_2O, 400 MHz.

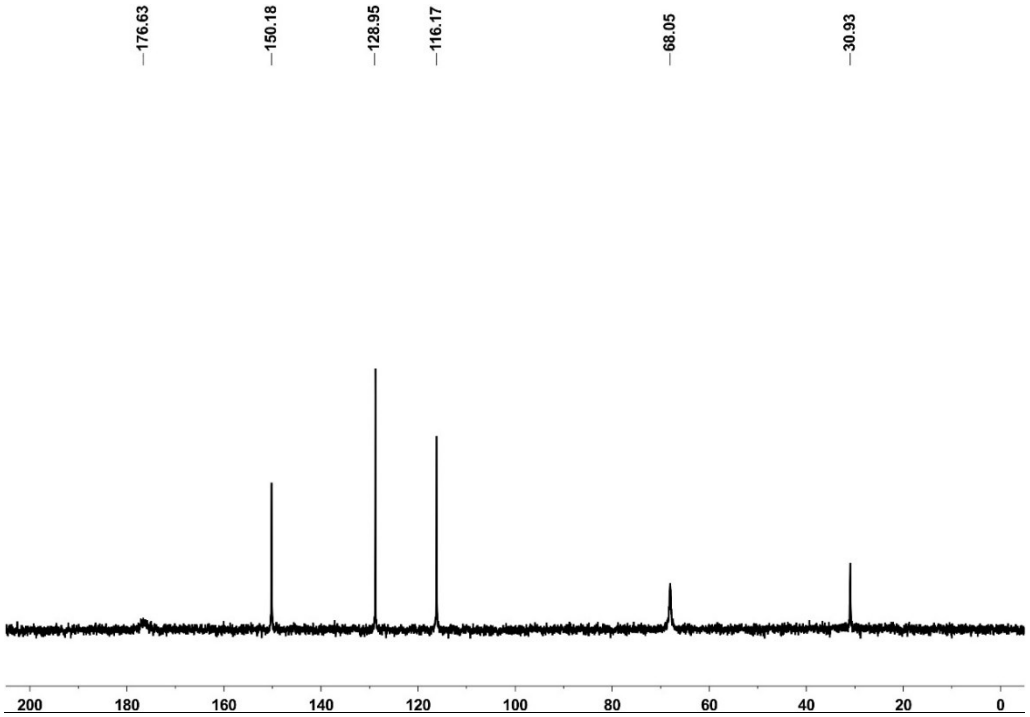

Fig. S6. ^{13}C NMR spectrum of CP6A in D_2O, 100 MHz.

3. Supporting results and experimental raw data

3.1 Additional ^{1}H NMR spectra of host-guest mixture.

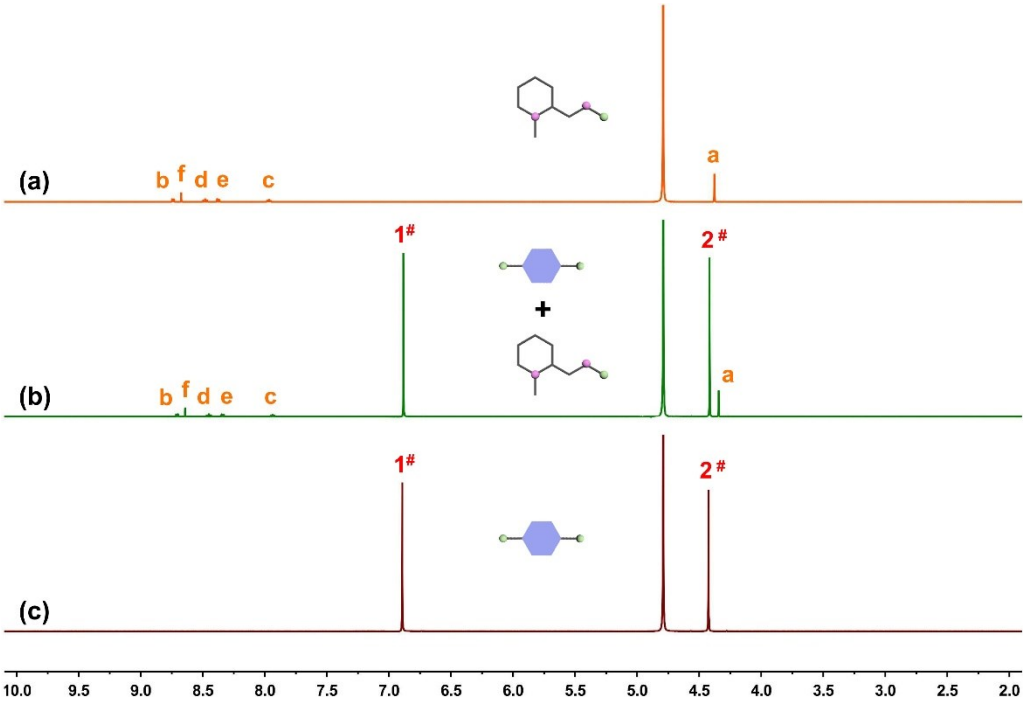

Fig. S7. ^{1}H NMR spectrum (400 MHz, D_2O) of (a) PAM (5 mM), (b) PAM (5 mM) + M (30 mM) and (c) M (30 mM).

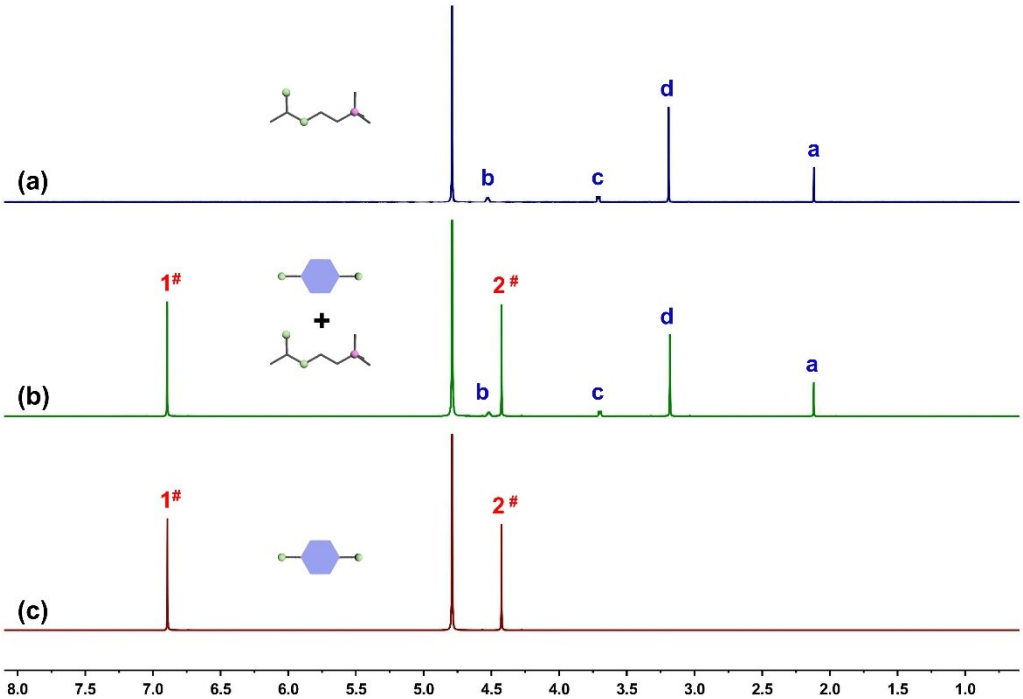

Fig. S8. ^{1}H NMR spectrum (400 MHz, D_2O) of (a) ACh (5 mM), (b) ACh (5 mM) + M (30 mM) and (c) M (30 mM).

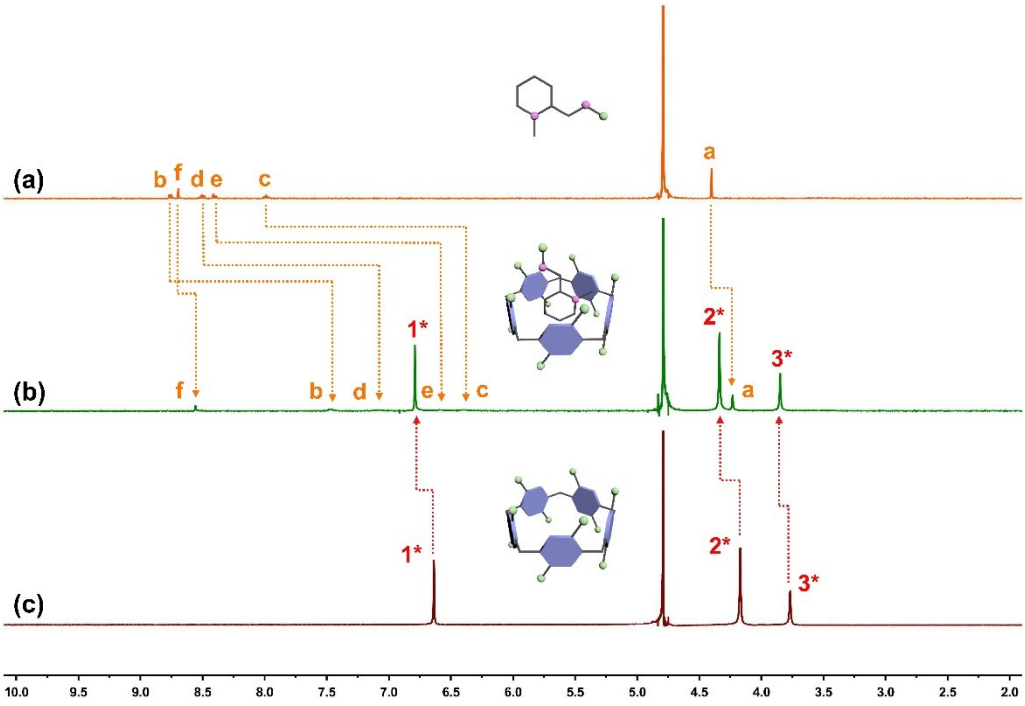

Fig. S9. ^{1}H NMR spectrum (400 MHz, D_2O) of (a) PAM (5 mM), (b) PAM (5 mM) + CP5A (5 mM) and (c) CP5A (5 mM).

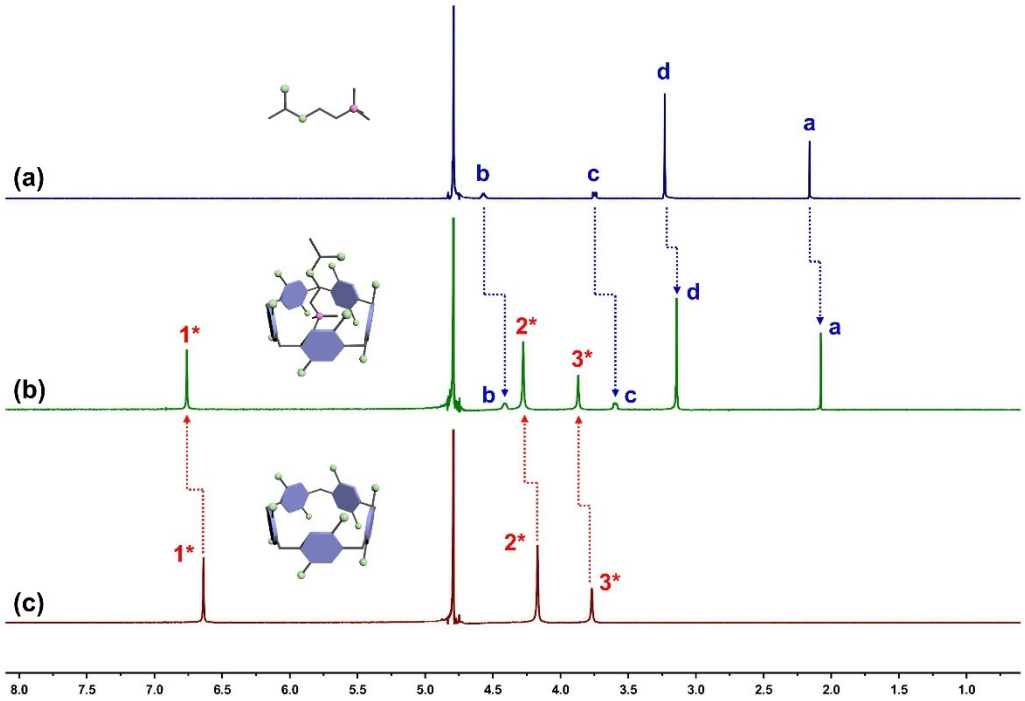

Fig. S10. ^{1}H NMR spectrum (400 MHz, D_2O) of (a) ACh (5 mM), (b) ACh (5 mM) + CP5A (5 mM) and (c) CP5A (5 mM).

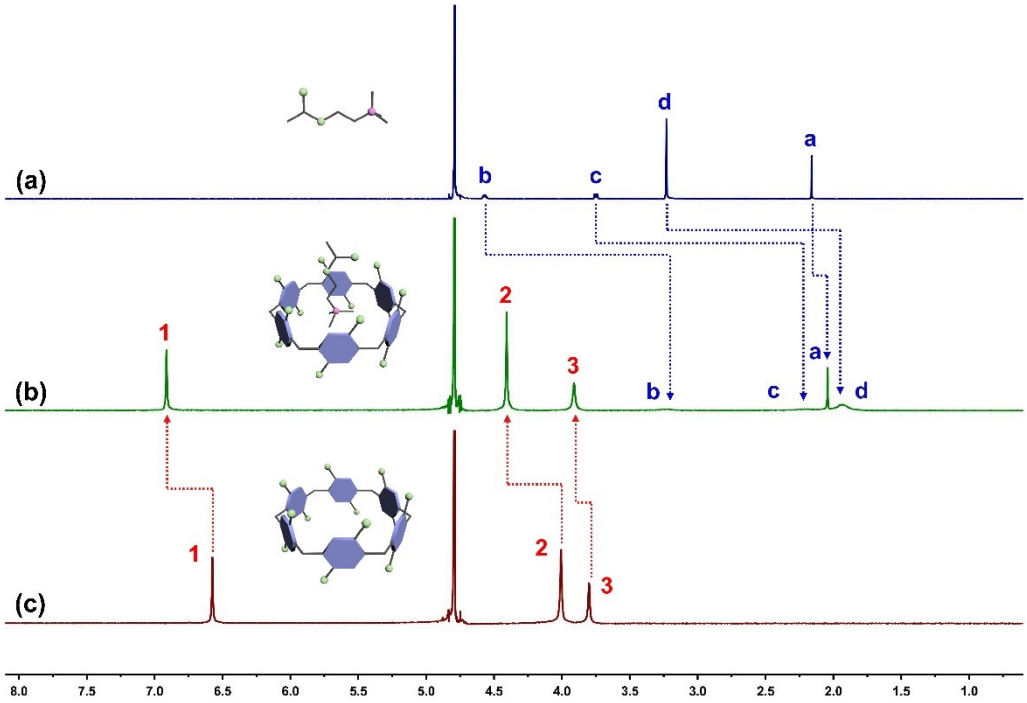

Fig. S11. ^{1}H NMR spectrum (400 MHz, D_2O) of (a) PAM (5 mM), (b) PAM (5 mM) + CP6A (5 mM) and (c) CP6A (5 mM).

3.2 Binding affinities between hosts and guests.

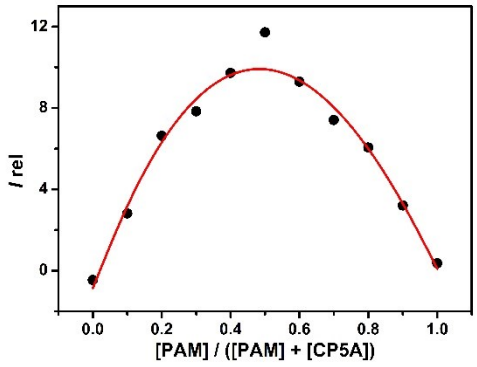

Fig. S12. Job's plot for CP5A with PAM in 10 mM PBS buffer at pH 7.4 (λ_{ex} = 290 nm, λ_{em} = 330 nm, [CP5A] + [PAM] = 2.00 μM).

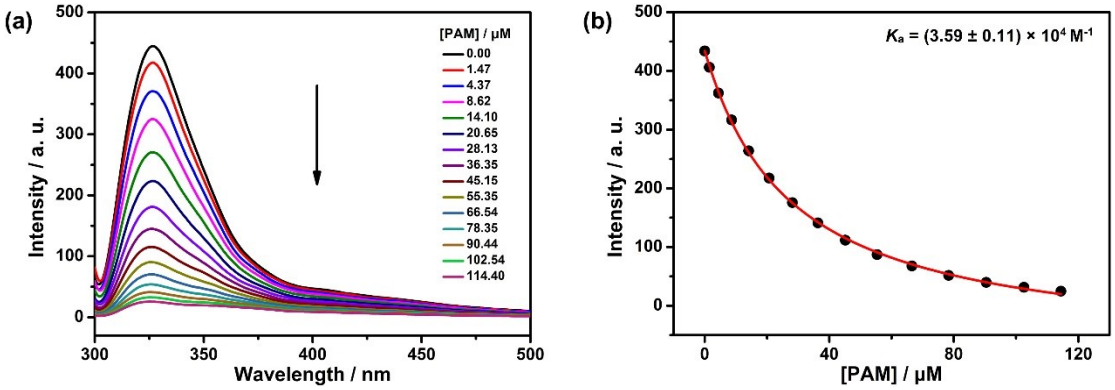

Fig. S13. (a)Fluorescence titration of CP5A (1.00 μM) with PAM in 10 mM PBS buffer at pH 7.4, λ_{ex} = 290 nm. (b) The associated titration curve at λ_{em} = 330 and fit according to a 1:1 binding stoichiometry. Data were from n =3 independent experiments and are presented as mean ± SD.

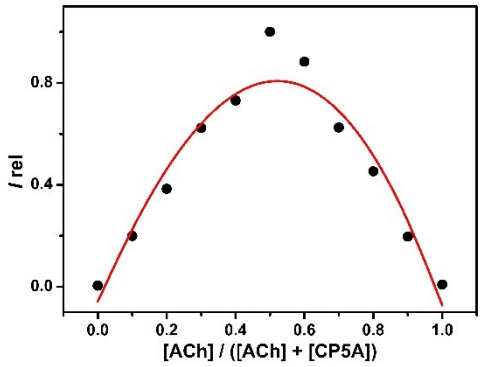

Fig. S14. Job's plot for CP5A with ACh in 10 mM PBS buffer at pH 7.4 (λ_{ex} = 290 nm, λ_{em} = 330 nm, [CP5A] + [ACh] = 10.00 μM).

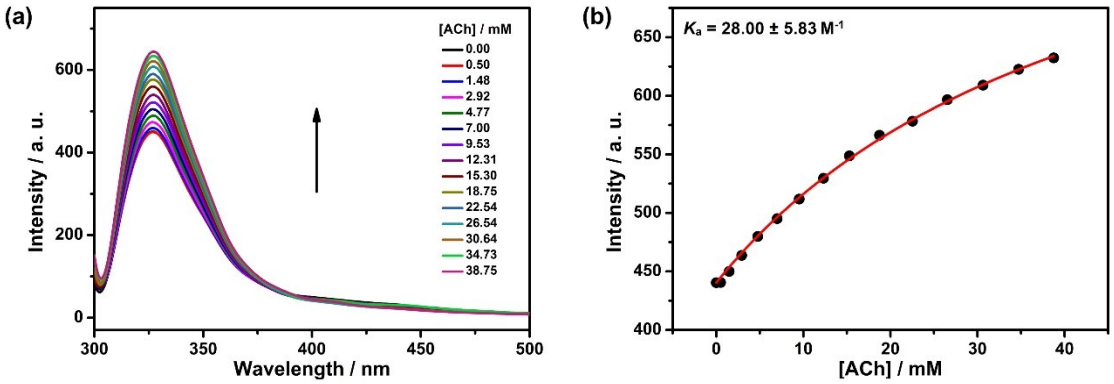

Fig. S15. (a) Fluorescence titration of CP5A (1.00 μM) with ACh in 10 mM PBS buffer at pH 7.4, λ_{ex} = 290 nm. (b) The associated titration curve at λ_{em} = 330 and fit according to a 1:1 binding stoichiometry. Data were from n =3 independent experiments and are presented as mean ± SD.

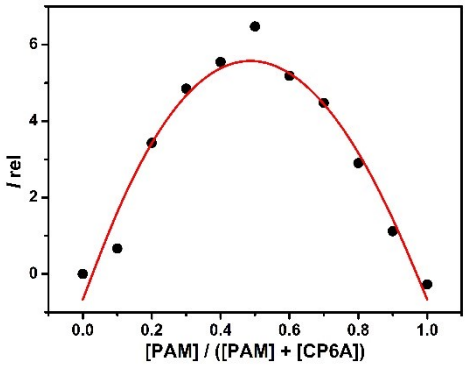

Fig. S16. Job's plot for CP6A with PAM in 10 mM PBS buffer at pH 7.4 (λ_{ex} = 290 nm, λ_{em} = 330 nm, [CP6A] + [PAM] = 2.00 μM).

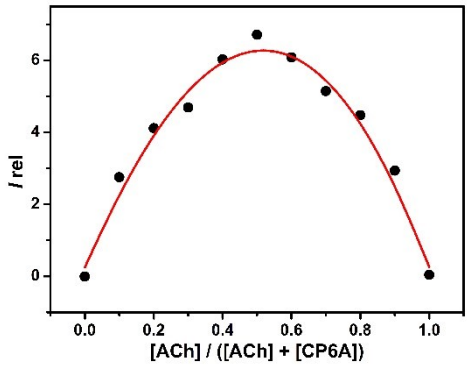

Fig. S17. Job's plot for CP6A with ACh in 10 mM PBS buffer at pH 7.4 (λ_{ex} = 290 nm, λ_{em} = 330 nm, [CP6A] + [ACh] = 2.00 μM).

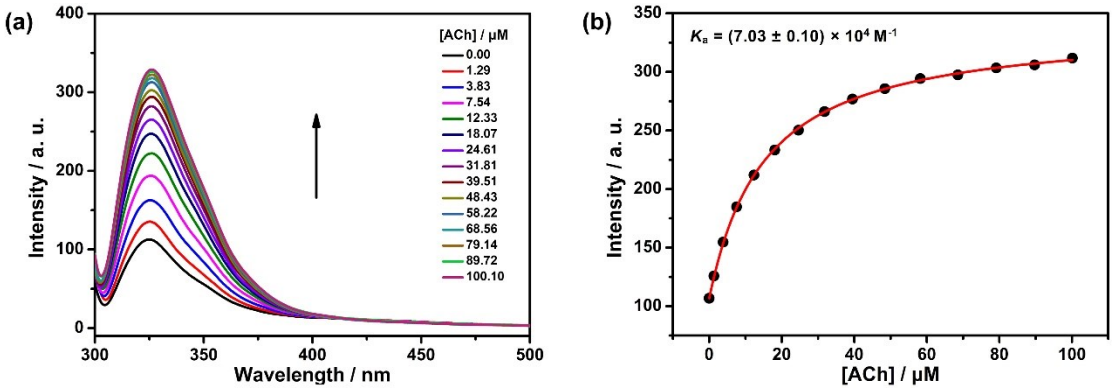

Fig. S18. (a) Fluorescence titration of CP6A (1.00 μM) with ACh in 10 mM PBS buffer at pH 7.4, λ_{ex} = 290 nm. (b) The associated titration curve at λ_{em} = 330 and fit according to a 1:1 binding stoichiometry. Data were from n =3 independent experiments and are presented as mean ± SD.

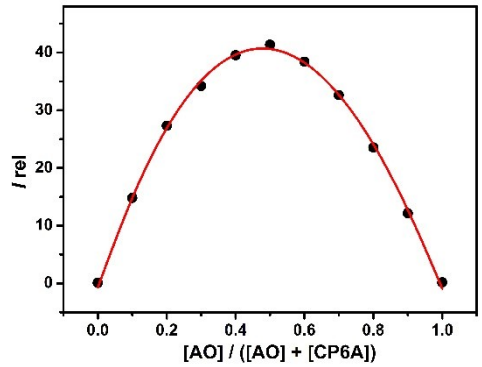

Fig. S19. Job's plot for CP6A with AO in 10 mM PBS buffer at pH 7.4 (λ_{ex} = 492 nm, λ_{em} = 523 nm, [CP6A] + [AO] = 2.00 μM).

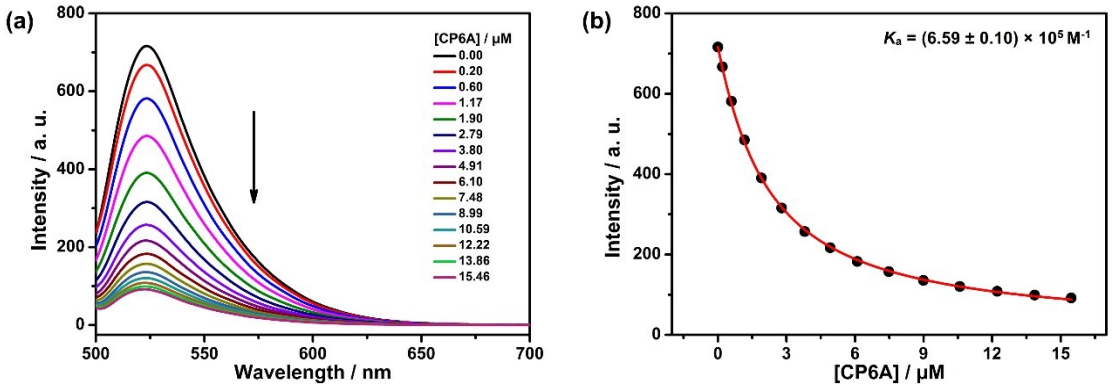

Fig. S20. (a) Fluorescence titration of AO (1.00 μM) with CP6A in 10 mM PBS buffer at pH 7.4, λ_{ex} = 492 nm. (b) The associated titration curve at λ_{em} = 523 and fit according to a 1:1 binding stoichiometry. Data were from n =3 independent experiments and are presented as mean ± SD.

3.3 Representative trace of nAChR (α7) currents.

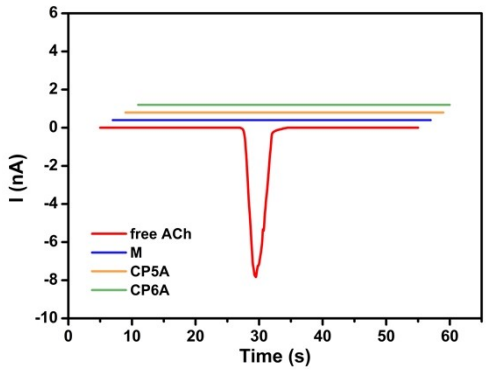

Fig. S21. Currents in response to ACh (30 μM), M (180 μM), CP5A (30 μM) and CP6A (30 μM) respectively. Currents were recorded with whole-cell patch-clamp electrophysiology from a HEK-293 cell expressing nAChRs (α7) and voltage-clamped to -70 mV.

3.4 Fluorescence quenching of AO by the complexion of CP6A and the corresponding recovery by the displacement of ACh.

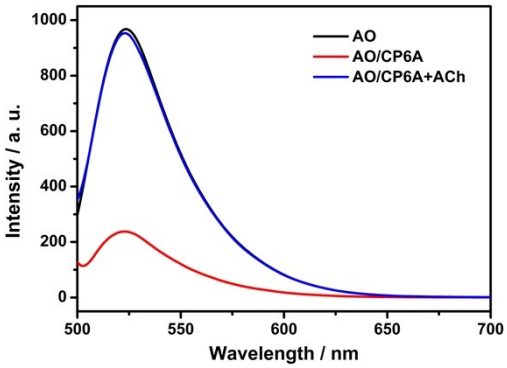

Fig. S22. Fluorescence spectra of AO (λ_{ex} = 492 nm, 10 μM), AO in the absence of 50 μM CP6A (red) and upon addition of 1 mM ACh (blue) in 10 mM PBS buffer at pH 7.4.

3.5 Statistical analysis of rats brain radiance after intracerebroventricular injection with AO/CP6A.

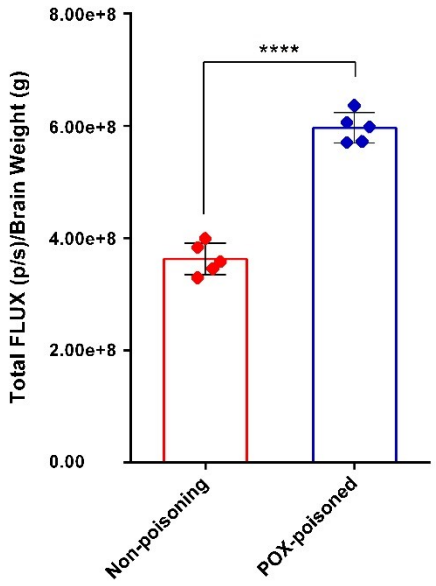

Fig. S23. Statistics analysis of *ex vivo* brain radiance. The total amount of Fluc activity was normalized to the weight of the individual brain. The data were presented as mean ± SD (n = 5). Significant differences were assessed using t test. ****$P < 0.0001$.

3.6 Cytotoxicity studies and histopathology of cerebral cortex and hippocampal region.

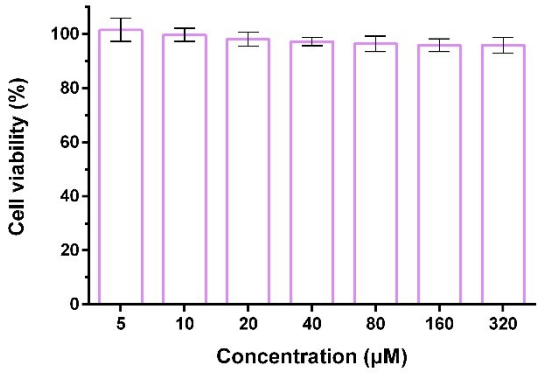

Fig. S24. Relative cell viabilities of bEnd.3 cells after incubation for 72 h with CP6A at the indicated concentrations. Cell death was then measured by using a CCK-8 assay (mean ± SD, n = 5).

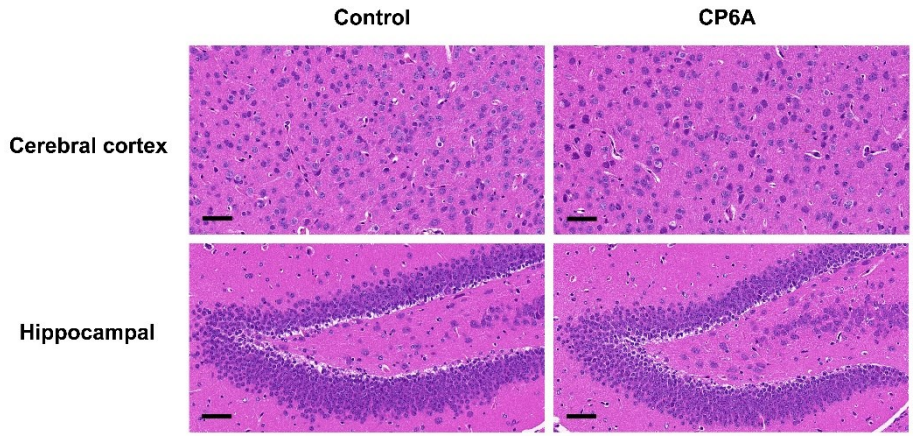

Fig. S25. Histopathologic analysis of the cerebral cortex and hippocampal region stained with H&E 72 h after treatment with PBS (control) and CP6A (scale bar: 100 μm).

3.7 The calibration curve for PAM.

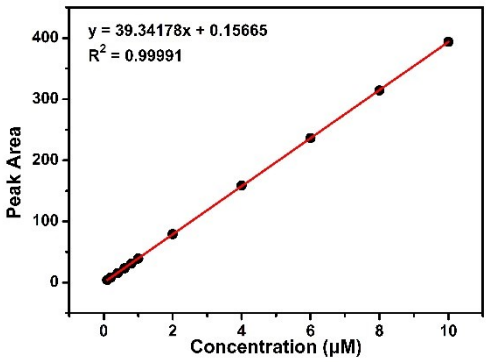

Fig. S26. Calibration curve obtained by HPLC and used for calculating the PAM concentration in the cerebrospinal fluid described in the main text.

3.8 Reactivation of brain AChE *in vivo*.

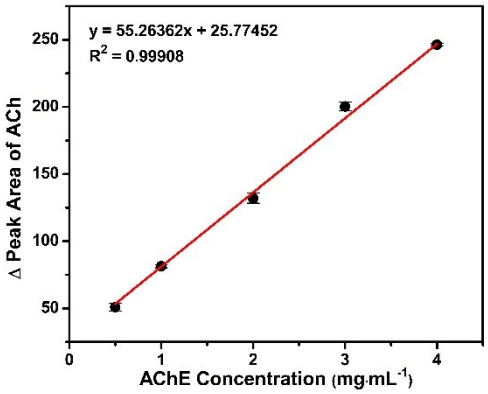

Fig. S27. Calibration curve obtained by HPLC and used for calculating the AChE concentration in brain homogenates described in the main text (mean ± SD, n = 3).

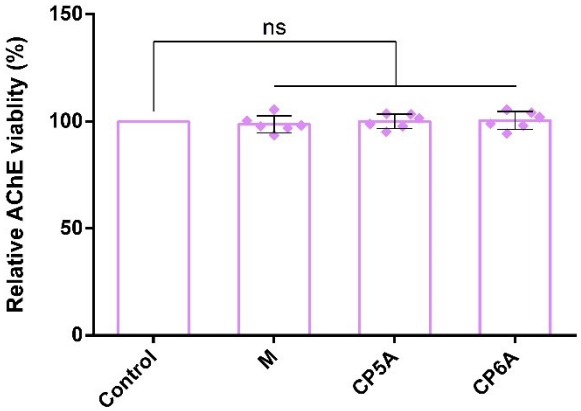

Fig. S28. Determination of brain AChE viability *in vivo*. Mean AChE activity of brain homogenates was measured in a control group of rats (taken as 100%) and after intranasal administration of M, CP5A and CP6A (mean ± SD, n = 6). Significant differences were assessed using one-way ANOVA tests with multiple comparisons; ns = not significant.

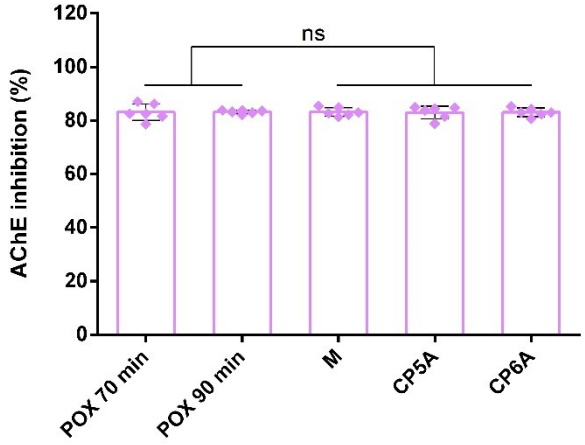

Fig. S29. Determination of brain AChE reactivation level *in vivo*. Mean AChE activity of brain homogenates was measured in a control group of rats (taken as 100%), after poisoning by 0.8 × LD_{50} of POX (600 μg·kg^{-1}, *i.p.*) and after intranasal administration of M, CP5A and CP6A (mean ± SD, n = 6). Significant differences were assessed using one-way ANOVA tests with multiple comparisons; ns = not significant.

3.9 Pharmacodynamics analysis.

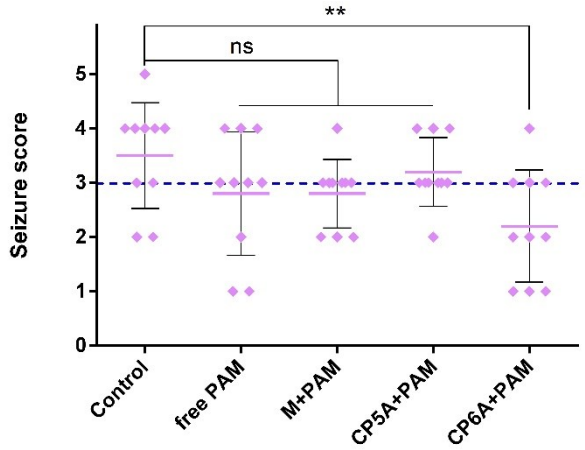

Fig. S30. Efficiency of several formulations against 2 × LD_{50} of POX-induced behavioural seizures. The graph showed the seizure score of rats, 7 min after intranasal administration of PBS, free PAM, M+PAM, CP5A+PAM and CP6A+PAM, respectively (mean ± SD, n = 10). Significant differences were assessed using one-way ANOVA tests with multiple comparisons. ns, not significant. *P < 0.05, **P < 0.01, ****P < 0.0001.

Table S1. Several groups protect rats against 2 × LD_{50} of POX

Group	SE onset time (min)	n/N (10 min)	n/N (24 h)
Control	6.10 ± 0.58	2/10	0/10
M	6.19 ± 1.53	1/10	0/10
CP5A	6.26 ± 0.75	2/10	0/10
CP6A	**7.10 ± 1.12**	**5/10**	**0/10**
free PAM	7.21 ± 1.12	7/10	1/10
M+PAM	7.32 ± 1.20	6/10	1/10
CP5A+PAM	6.93 ± 1.00	4/10	0/10
CP6A+PAM	**9.13 ± 1.12**	**8/10**	**5/10**

[a]n is the number of rats survival after challenge. N is total number of rats in the group.

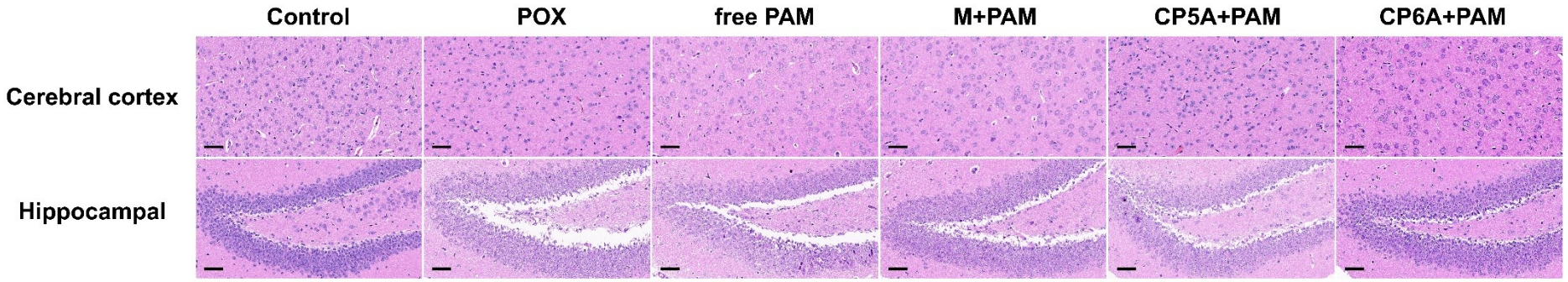

Fig. S31. Histopathologic analysis of the cerebral cortex and hippocampal region stained with H&E after poisoning by 2 × LD_{50} of POX (1500 μg·kg^{-1}, *i.p.*) and after intranasal administration of PBS (control), free PAM, M+PAM, CP5A+PAM and CP6A+PAM; the dose of PAM was 10 mg·kg^{-1} (scale bar: 100 μm).

References

[1] J. Chen, Y. Zhang, Z. Meng, L. Guo, X. Yuan, Y. Zhang, Y. Chai, J. L. Sessler, Q. Meng, C. Li, *Chem. Sci.* **2020**, *11*, 6275-6282.

[2] Q. Zhou, Y. Zhang, J. Du, Y. Li, Y. Zhou, Q. Fu, J. Zhang, X. Wang, L. Zhan, *ACS Nano* **2016**, *10*, 2678-2692.

[3] R. J. Racine, *Electroencephalogr. Clin. Neurophysiol*. **1972**, *32*, 281-294.

[4] C. Li, X. Shu, J. Li, S. Chen, K. Han, M. Xu, B. Hu, Y. Yu, X. Jia, *J. Org, Chem.,* **2011**, *76*, 8458-8465.